HEFAT2011
8th International Conference on Heat Transfer, Fluid Mechanics and Thermodynamics
11 – 13 July 2011
Pointe Aux Piments, Mauritius

EXPERIENCE WITH THE LARGE EDDY SIMULATION (LES) TECHNIQUE FOR THE MODELLING OF PREMIXED AND NON-PREMIXED COMBUSTION

W. Malalasekera
Wolfson School of Mechanical and Manufacturing Engineering, Loughborough University
Loughborough, Leics, LE11 3TU, UK.
w.malalasekera@lboro.ac.uk
S.S. Ibrahim
Department of Aeronautics and Automotive Engineering, Loughborough University, Loughborough Leics, LE11 3TU, UK
s.s.ibrahim@lboro.ac.uk
A.R. Masri
School of Aerospace Mechanical and Mechatronic Engineering
University of Sydney
Sydney, NSW 2006, Australia.
S. R. Gubba
CFD centre, School of Process, Environment and
Materials Engineering, University of Leeds, Leeds, LS2 9JT, UK
S.R.Gubba@leeds.ac.uk
S. K. Sadasivuni
Wolfson School of Mechanical and Manufacturing Engineering, Loughborough University
Loughborough, Leics, LE11 3TU, UK.

ABSTRACT

Compared to RANS based combustion modelling, the Large Eddy Simulation (LES) technique has recently emerged as a more accurate and very adaptable technique in terms of handling complex turbulent interactions in combustion modelling problems. In this paper application of LES based combustion modelling technique and the validation of models in non-premixed and premixed situations are considered. Two well defined experimental configurations where high quality data are available for validation is considered as case studies to demonstrate the methods, accuracy and capability of the LES combustion modelling technique as a predictive tool. The large eddy simulation technique for the modelling flow and turbulence is based on the solution of governing equations for continuity and momentum in a structured Cartesian grid arrangement. Smagorinsky eddy viscosity model with a localised dynamic procedure is used as the sub-grid scale turbulence model. A swirl flame is considered as the non-premixed combustion application. For non-premixed combustion modelling a conserved scalar mixture fraction based steady laminar flamelet model is used. A radiation model incorporating the discrete transfer method is also included in the non-premixed swirl flame calculations. For premixed combustion where the application considered here is flame propagation in a confined explosion chamber, a model based on dynamic flame surface density (DSFD) is used. It is shown that in both cases LES based combustion models perform remarkably well and results agree well with the experimental data.

INTRODUCTION

Computational Fluid Dynamics is now widely used for the modelling and design of combustion systems. To this end Computational Fluid Dynamics (CFD) has become a vital tool in the design process and more and more industries are now using CFD to explore flow behaviour of various designs and simulate temperature, heat transfer and emissions in combustion equipment before prototypes are built for testing. It allows the designers to conduct numerous parametric studies to fine-tune flow and combustion conditions of their designs and shorten expensive experimental testing phase of product development. Until recently Reynolds Averaged Navier-Stokes (RANS) techniques combined with combustion models have been used for CFD modelling of combustion systems. However, the ability of RANS based techniques to predict complex flow situations where swirl and transient effect are dominant has been limited due to the form of modelling involved in RANS techniques. Large Eddy Simulation (LES) technique uses a completely different approach to RANS and attempts to solve for transient flow features of large eddies of the flow and therefore it has been shown that LES is capable of resolving more complex turbulent flows better than RANS.

There are many issues that make combustion modelling one of the most difficult areas in CFD applications. Complexities such as turbulence/chemistry interactions, chemical kinetics, coupling of flow turbulence and temperature to density, heat transfer and radiation effects make the CFD modelling of combustion very challenging. The interaction of turbulence and chemistry plays an important role in premixed as well as non-premixed combustion situations. Therefore success in combustion modelling in many situations depends on the

success in turbulence modelling. Until recently RANS based flow models coupled with various types of combustion models to suit the application area have been used with some success in industrial applications. However in more complex situations such as strong swirling flows and highly dynamics propagating flames, success of the RANS based models has been limited. This paper summarises application of LES based combustion modelling techniques to cases where RANS based modelling has resulted in limited success due to complexity of the flow configuration. For premixed combustion simulations, a propagating flame in a confined explosion chamber with obstacles is considered. For non-premixed, the application of LES for the modelling of a swirl stabled flame is considered. For both cases experimental data sets for validation have been obtained from the experiments conducted at the Sydney University.

Modelling of Swirl Flames

Swirl stabilised turbulent flames are widely used in a range of practical combustion applications such as gas turbines, furnaces, power station combustors and boilers. The complexity of the resulting flames in swirl flame situations depend on the strength of swirl and the method of swirl generation. Modelling of and accurate prediction of such complex details remains a challenge and LES based CFD and combustion modelling techniques have various advantages over RANS based models. Numerical calculation of swirl flows has been undertaken in several previous studies. Majority of the attempts have used Reynolds averaged Navier-Stokes (RANS) equations accompanying different turbulence models to predict swirl flows. Reviews by Sloan et al. [1] and Weber et al. [2] have summarised these attempts. In generals RANS based models are primarily suitable to calculate stationary flows with non-gradient transport and they are not capable of capturing the unsteady nature of the large-scale flow structures found in swirl flows. As large eddy simulation (LES) technique solves for large scale unsteady behaviour of turbulent flows it is a promising numerical tool to predict complex swirling turbulent flows. Among others, the studies of Kim et al.[3], Sankaran and Menon [4], Di Mare et al. [5], Wall and Moin [6] have demonstrated the ability of LES to capture detailed flow field in swirling flow configurations.

Modelling of Propagating Premixed Flames

Premixed combustion is encountered in many engineering applications such as spark ignition engines, gas turbines and accidental explosion events. In these flow situations outstanding research issues associated with understanding the structure of the flame front and the combustion regimes as the flame front propagates through highly turbulent flow field are further complicated by instabilities, which occur due to the unsteady nature of the flow. Understanding such issues is central to the development of advanced physical sub-models that improve current predictive capabilities for turbulent premixed flames. Here we consider a laboratory scale experimental vented explosion situation and apply the large eddy simulation technique to predict experimentally obtained data. Previous applications of RANS based models to the same geometrical configuration have shown the limitations of RANS based models [7]. LES based models are now accepted as feasible computational tools in modelling propagating premixed turbulent combustion problems [8-12]. LES has a clear advantage over classical Reynolds averaged methods in the capability of accounting for time-varying nature of flows and this is particularly important in transient processes such as turbulent premixed propagating flames. Ever increasing speed of processors and the availability of parallel computing hardware make the LES technique a very useful tool for accurate modelling of highly turbulent combusting flows, such as propagating premixed flames.

NUMERICAL METHOD

Equations solved

LES technique attempts to resolves the large scale turbulent motions which contain the majority of turbulent kinetic energy and control the dynamics of turbulence. Unresolved small scales or sub-grid scales are modelled. However when applied to combusting flows, the advantage of resolving the large scale motion is not applicable to chemical source term, as the chemical time scales are much smaller and therefore combustion needs to be modeled separately. Most combustion models rely on accurate prediction of turbulent quantities and the resulting mixing field. LES still seems to have the advantages over RANS due to its ability to predict more accurately (compared to RANS) the intense scalar mixing process in most complex flows.

In LES the governing equations which resolve the large scale features are obtain by applying a filtering operator. A number of filters are used in LES and a top hat filter having the filter-width $\overline{\Delta}_j$ set equal to the size Δx_j of the local cell is used in the present work. The transport equations for Favre filtered mass, momentum are given by:

$$\frac{\partial \overline{\rho}}{\partial t} + \frac{\partial \overline{\rho}\widetilde{u}_j}{\partial x_j} = 0 \tag{1}$$

$$\frac{\partial \overline{\rho}\widetilde{u}_i}{\partial t} + \frac{\partial (\overline{\rho}\widetilde{u}_i\widetilde{u}_j)}{\partial x_j} = -\frac{\partial \overline{P}}{\partial x_i} + \frac{\partial}{\partial x_j}\left[\overline{\rho}\nu\left(\frac{\partial \widetilde{u}_i}{\partial x_j} + \frac{\partial \widetilde{u}_j}{\partial x_i}\right) - \frac{2}{3}\overline{\rho}\frac{\partial \widetilde{u}_k}{\partial x_k}\right] + \frac{\partial \tau_{ij}}{\partial x_j} \tag{2}$$

Turbulence Model

The sub-grid contribution to the momentum flux is computed using Smagorinsky eddy viscosity model [13] which uses a model constant C_s, the filter width $\overline{\Delta}$ and strain rate tensor $S_{i,j}$ according to equation (3):

$$\nu_t = C_s\overline{\Delta}^2\left|S_{i,j}\right| = C_s\overline{\Delta}^2\left|\frac{1}{2}\left(\frac{\partial \widetilde{u}_i}{\partial x_j} + \frac{\partial \widetilde{u}_j}{\partial x_i}\right)\right| \tag{3}$$

In the present work the model parameter C_s is obtained through a localised dynamic procedure depending on the application [14,15].

Combustion Model: Non-premixed

In combustion, the chemical reactions occur mostly in the sub-grid scales and therefore consequent modelling is required for combustion chemistry. In this work the Steady Laminar Flamelet Model (SLFM) is used to form the combustion modelling aspect. Here a presumed probability density function (PDF) of the mixture fraction is chosen as a means of modelling the sub-grid scale mixing. The transport equation for conserved scalar mixture fraction is written as

$$\frac{\partial \overline{\rho}\widetilde{f}}{\partial t}+\frac{\partial}{\partial x_j}\left(\overline{\rho}\widetilde{u}_j\widetilde{f}\right)=\frac{\partial}{\partial x_j}\left[\overline{\rho}\left(\frac{\nu}{\sigma}+\frac{\sigma_t}{\sigma_t}\right)\frac{\partial \widetilde{f}}{\partial x_j}\right] \quad (4)$$

In the above equations ρ is the density, $\widetilde{u}_i$ is the velocity component in x_i direction, p is the pressure, ν is the kinematics viscosity, f is the mixture fraction, ν_t is the turbulent viscosity, σ is the laminar Schmidt number, σ_t is the turbulent Schmidt number. A β function is used for the mixture fraction PDF. The functional dependence of the thermo-chemical variables is closed through the steady laminar flamelet approach. In this approach the variables, density, temperature and species concentrations only depend on Favre filtered mixture fraction, mixture fraction variance and scalar dissipation rate. The sub-grid scale variance of the mixture fraction is modelled assuming the gradient transport model proposed by Branley and Jones [16]. In this work the flamelet calculations have been performed using the Flamemaster code [17] incorporating the GRI 2.11 mechanism for detailed chemistry. Further details can be found in Malalasekera et al. [18].

Many combustion simulations tend to ignore the effect of radiation in the calculations. This is because the governing radiative transfer equation is of integro-differential nature makes the analysis difficult and computationally expensive. The well-known Discrete Transfer Method [19], is used as the radiation calculation algorithms in this work. This is a ray-based calculation method and in our previous work we have established the accuracy and advantages of this method when applied to large and complex problems [20,21]. The absorption coefficient is calculated from LES data using transient temperature and relevant species distributions. For this the Mixed Grey Gas Model of Truelove [22], is used in the present study. The major computational effort in the discrete transfer method is to trace rays through cell volumes in the descretised radiation space. An efficient and fast ray calculation algorithm used in our previous studies [20,21] is employed in this work. Although transient calculation of radiation is computationally very expensive the algorithm we use is devised in such a way that ray data are calculated only once and stored to re-use in each radiation calculation at every time step with updated temperature and absorption coefficient data.

Combustion model: Premixed

As mentioned above, in LES, large eddies above a cut-off length scale are resolved and the small ones are modelled by assuming isotropic in nature, using sub-grid scale (SGS) models. For premixed combustion simulations presented here Favre filtered (density weighted) conservation equations of mass, momentum, energy and a transport equation for the reaction progress variable are solved together with the state equation. Turbulence is modelled using the classical Smagorinsky model [13] and the model coefficient is calculated from instantaneous flow conditions using the dynamic determination procedure developed by Moin et al. [15], for compressible flows.

In the application considered here modelling of the mean chemical reaction rate in deflagrating flames is very challenging due to its non-linear relation with chemical and thermodynamic states, and often characterised by propagating thin reaction layers thinner than the smallest turbulent scales. The major difficulty in the modelling of reaction rate is due to sharp variation of thermo chemical variables through the laminar flame profile, which is typically very thin [23]. This issue is strongly affected by turbulence, which causes flame wrinkling and thereby forming the most complex three way thermo-chemical-turbulence interactions. However, assuming single step irreversible chemistry and the Zeldovich instability (thermal diffusion), i.e. unity Lewis number will reduce the complexity of the whole system. The chemical state is then described by defining the reaction progress variable $\widetilde{c}$ from zero to one in unburned mixture and products respectively, based on fuel mass fraction. Mathematically it can be derived as, $1-Y_{fu}/Y_{fu}^0$. Here Y_{fu} is the local fuel mass fraction and Y_{fu}^0 is the fuel mass fraction in unburned mixture. The mean SGS chemical reaction rate $\overline{\dot{\omega}}_c$ in the reaction progress variable equation (not shown here) is modelled by following the laminar flamelet approach as:

$$\overline{\dot{\omega}}=\rho_u u_L \overline{\Sigma} \quad (5)$$

where ρ_u is the density of the unburned mixture, u_L is the laminar burning velocity, and $\overline{\Sigma}$ is the flame surface density. Flame surface density models have been used in the RANS context to predict similar premixed combustion problems [7]. Here this approach is extended to LES. In this work the LES combustion model is based on dynamic determination of the resolved and unresolved flame surface density (FSD), which allows for the sub-grid scale (SGS) dynamic effects of the local flame interactions. Following the authors' recent work [24,25] a novel dynamic flame surface density (DFSD) [26], is used for premixed combustion modelling work described here to calculate the reaction rate given by equation (5). Further details are available in Ibrahim et al. [25].

EXPERIMENTAL AND COMPUTATIONAL DETAILS

For the validation of both premixed and non-premixed combustion models used here we use experiments conducted at the Sydney University. Two experimental datasets are considered. (1) Swirl burner experiment [27,28] and (2) explosion deflagrating flames experiments by Kent et al. [29].

Sydney Swirl Burner

Sydney swirl flame experiments provide a high quality experimental database for the validation of computations [27,28]. Figure 1 (a) shows the experimental configuration of the Sydney swirl burner. The burner has a 3.6mm diameter

central jet with a 50mm diameter bluff body surrounding it. Swirl flow generated downstream by means of inclined radial jets enters the burner level through an annulus around the bluff body as shown in the figure. The swirl annulus covers the bluff body with an outer diameter of 60mm. The entire burner is placed in a tunnel with an air flow with low velocity. This enables the modellers to set very well defined boundary conditions in their computations. The dimensions of the tunnel are 250 x 250 (mm). From this experimental series flames known as SMH1 and SMH2 are the two flames widely used for validation of combustion simulations in swirl flames. These two flames have the same burner configuration, but different flow conditions. Detail description of the burner parameters and its operation is available in the above references. The SMH1 flame with flame operating conditions shown in Table 1 is considered for the present calculations. In this flame the fuel jet consists of CH4/H2 with an inlet jet velocity (U_j) of 140.8 m/s. A swirl number of 0.32 is maintained for the swirl inlet with an axial velocity (U_s) and tangential velocity (W_s) components of 42.8 m/s and 13.8 m/s respectively. The external ambient co-flow velocity of 20 m/s (U_e) is provided.

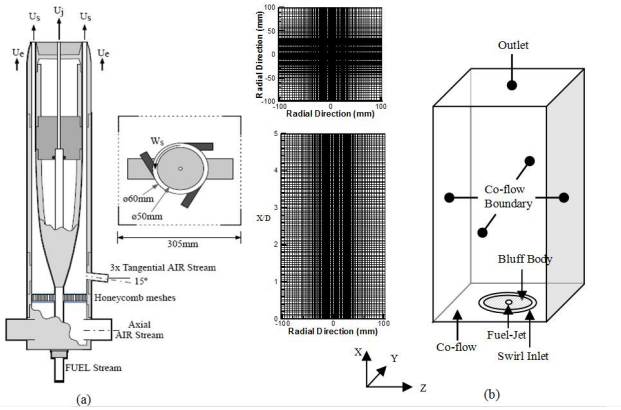

Figure 1. Experimental configuration and computational geometry.

The computational geometry and grid details used in LES calculations are depicted in the Figure 1(b). The computational domain has dimensions of 200 x 200 x 250 (all dimensions are in mm). The axial distance of approximately 70 jet diameters and the burner width of approximately 55 jet diameters are used in order to account the independency of flow entrainment from the surroundings. The inlet jet velocity is specified with a 1/7th power law profile. A Cartesian staggered non-uniform grid distribution of 100 x 100 x 100 in the X, Y and Z directions is used to discretise the domain.

Case	U_j	U_s	W_s	Re_j	S
SMH1	140.8	42.8	13.8	19300	0.32

Table 1: SMH1 properties

Sydney Experimental Explosion Chamber

The experimental test cases used to validate the LES predictions of explosion deflagrating flames are those, reported by The University of Sydney combustion group [29]. A schematic diagram of the laboratory scale explosion rig, with baffle plates and a solid square obstacle is illustrated in Fig. 2. The chamber is made of 50 mm square cross section with a length of 250 mm and having a total volume of 0.625 litres. This chamber has the capability to hold a deflagrating flame in a strong turbulent environment, generated due to the presence of solid obstacles at different downstream locations from the bottom ignition end. It is designed in such a way that locations of the baffle plates could be varied to construct several configurations of baffle arrangements with the standing square solid obstacle in the path of the deflagrating flame. These baffle stations are named as S1, S2 and S3 and located at 20, 50 and 80 mm respectively from the ignition point as shown in Fig. 2.

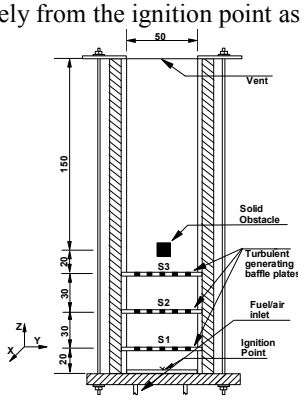

Figure 2

Family name	Configurations and order
Family 1	5 – 2 – 1
Family 2	1 – 7 – 4
Family 3	2 – 3 – 4
Family 4	6 – 7 – 0

Table 2 – Families of configurations

Each baffle plate is of 50 x 50 mm, aluminium frame, constructed from 3 mm thick sheet, consisting of five 4 mm wide bars each with a 5 mm wide space spreading them throughout the chamber. A solid square obstacle of 12 mm cross-section is centrally located at 96 mm from the bottom ignition end of the chamber. Depending on the location, the number of baffles and their positions, configurations shown in Fig. 3 have been used in the experiments. To aid the analysis and the discussion of the results various families of these configurations have been identified. Table 2 below shows a number of families that could be categorised. Simulation results for family 1 and 3 are presented and discussed briefly in this paper. Configuration 0 is the basic or trivial configuration without any obstacle plates. This configuration is also considered in the simulations.

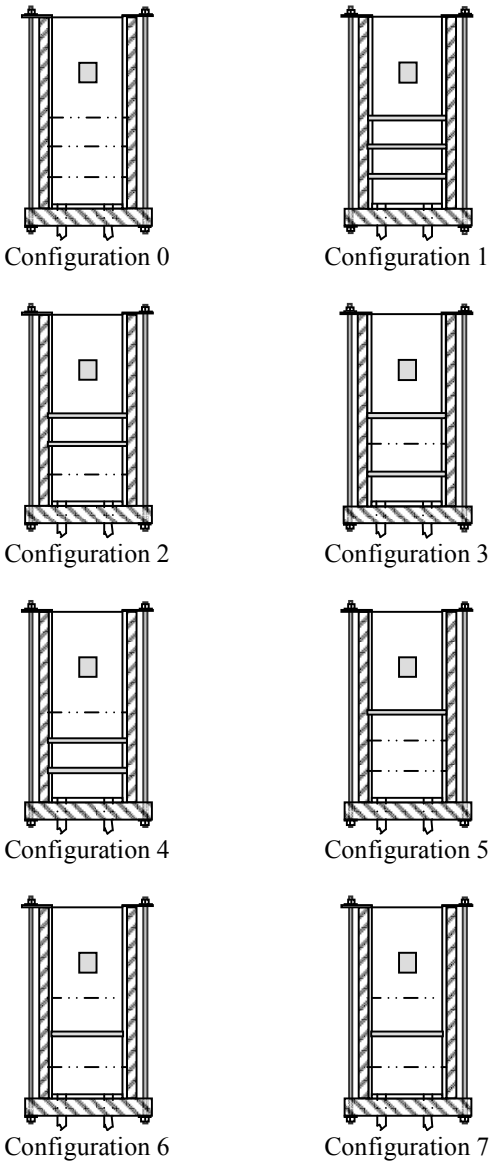

Figure 3 All configurations

RESULTS AND DISCUSSION

LES Modelling of Non-premixed Swirl Combustion : SMH1 Flame

This section presents sample of results from various numerical simulations performed for the SMH1 swirl flame. In order to identify the resulting differences between inclusion and non-inclusion of radiation, simulations were performed with and without radiation. In the discrete transfer method 16x16 number of rays were used for angular discretisation. Coupling of radiation with the laminar flamelet model was achieved by incorporating the enthalpy defect technique previously used in other RANS based calculations [30,31].

LES simulation including radiation is identified as NAFM (non adiabatic flamelet model) and the calculation without radiation is identified as AFM (adiabatic flamelet model). It should be noted that both models are based on the steady laminar flamelet model for non-premixed combustion.

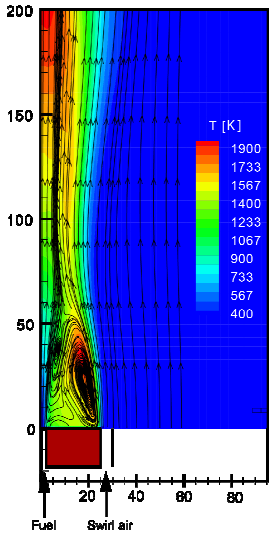

Fig. 4 Stream traces of axial velocity plotted with temperature contours at the central plane

Swirl flames exhibits complex flow features in terms of various recirculation zones and these features are important in flame stabilization. Fig. 4 shows the LES predicted mean flow pattern with stream traces of axial velocity plotted on temperature contours. Numerical results correctly predict two bluff body recirculation zones. These two counter rotating vortex zones lead to a high temperature region above the bluff body. Detailed results are presented for velocity flow field, temperature, mixture fraction and species mass fractions and compared with respective experimental data. Comparison of predicted axial and swirl velocity components compared with the experiments at various axial locations are shown in Fig. 5 and 6. It can be seen that LES results agree well with the experimental data indicating that overall flow features in this complex swirl flow situation have been predicted well by the LES based combustion model. LES resolves the axial velocity component very well at all locations except at one downstream location z/D=2.5. This location corresponds to the axial vortex breakdown region of this swirl flame and therefore flow is highly unstable. Because of this highly unstable nature current LES technique does not completely capture the exact flow and flame properties and this could well be a result of the deficiencies of the steady laminar flamelet concept which does not include transient, extinction and re-ignition effects. In Fig 6 the correct development of the swirl velocity pattern at radial distance of r/R = {1.0-1.2} at the initial three axial locations are captured well with both combustion models (NAFM and AFM). However, the discrepancies in the predictions can be found at further downstream locations. Again these discrepancies correspond to the highly unstable and transient region of the flame. Comparison of the results of NAFM and AFM shows that the effect of radiation on the flow field is minor. There are slight differences between inclusion and non-inclusion of radiation. Predictions with radiation show slightly closer agreement at most locations.

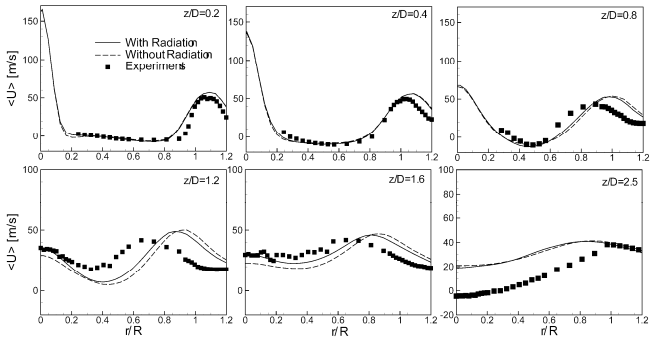

Fig. 5 Radial plot for axial velocity at different axial locations

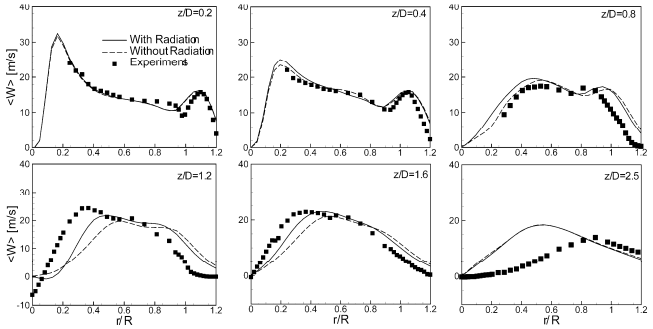

Fig. 6 Radial plot for swirl velocity at different axial locations

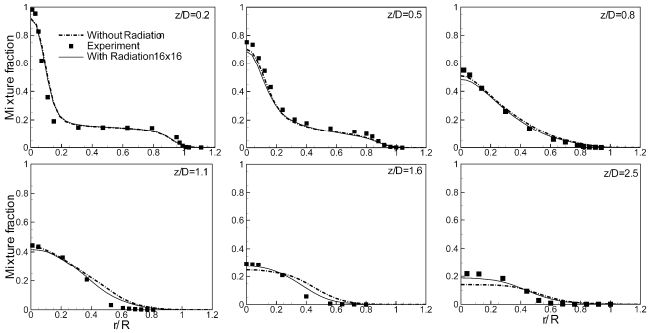

Fig. 7 Radial plot for mixture fraction at different axial locations

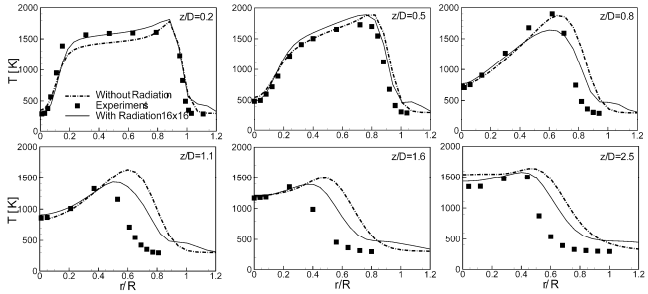

Fig. 8 Radial plot for temperature at different axial locations

Performance of NAFM and AFM model are further assessed through the comparison with other experimental data. Fig. 7 shows the predictions of mean mixture fraction from both models compared with measurements. The figure shows very close agreement with the experiments and both models show very similar results. Results including radiation show slightly better agreement at downstream locations.

Predicted radial profiles of mean temperature at various axial locations are compared in Fig. 8. Here inclusion of radiation shows a clear difference. It can be seen that NAFM which include radiation effects predict closer agreement than the AFM (without radiation). There is noticeable difference between the two results. Both models tend to over predict at downstream locations but NAFM with the radiation heat losses predict slightly closer to the experiments. It could be said that inclusion of radiation in LES calculation improves the overall quality of the results. At downstream axial locations radiation losses result in a drop in temperatures when compared with the adiabatic model hence the predictions are much closer to the measurements.

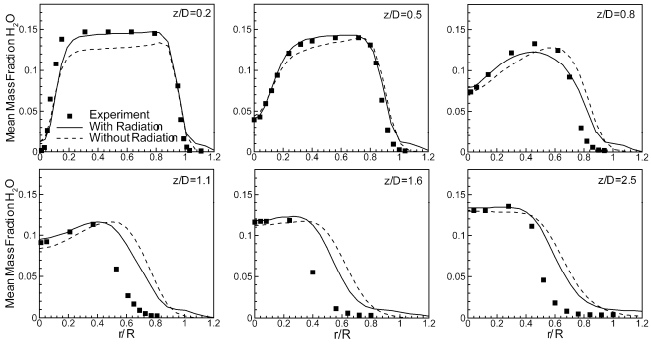

Fig. 9 Radial plot for mean mass fraction of H_2O at different axial locations

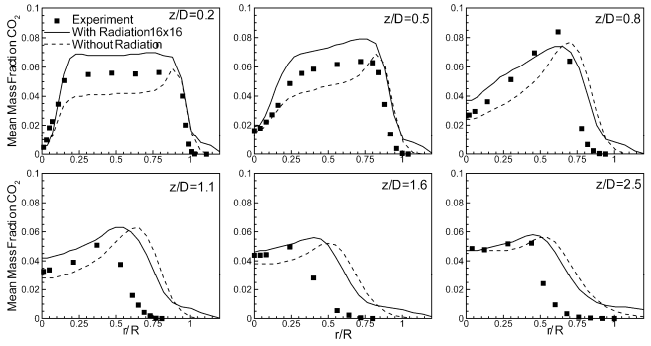

Fig. 10 Radial plot for mean mass fraction of CO_2 at different axial locations

Figures 9 and 10 show the predictions of mass fraction of H_2O and CO_2 respectively compared with experiments. Fig. 9 shows H_2O radial mass fractions. It can be seen that predictions with the NAFM model which include radiation are better than the AFM results. Similar observation can be made in CO_2 predictions (Fig. 10). At first three locations under prediction of CO_2 profiles seen with the AFM are much improved with NAFM calculations. Although they are slightly over-predicted at downstream locations, NAFM shows better agreement with the experimental data.

In general LES results show quite good agreement with experimental results and show the ability of the technique in predicting flame properties of this complex swirl flow situation. As mentioned there are still some deficiencies in the model. These could be due to various reasons. Improvements to sub-

grid scale combustion modelling and more fine grid resolutions for LES can possibly improve these. It is fair to note that the laminar flamelet model may not be the ideal model to use in highly turbulent dynamic situations. Transient flamelet models or models that incorporate extinction and re-ignition effects incorporated into LES could provide better results than the present calculations. However, the present calculations demonstrate that LES as a combustion modelling technique is quite successful and very useful for complex flow configurations.

LES Modelling of Premixed Propagating Flame over Obstacles

Results from the LES simulations of stagnant, stoichiometric propane/air deflagrating flames over solid obstacles are presented and discussed in this section. A novel DFSD model [25, 26] to account for the SGS chemical reaction rate is used to model premixed combustion in the vented chamber geometries shown in Fig. 3. Four families as identified in Table 2 were analysed for flame dynamics, structure and other combustion characteristics. In each case baffle plates and the solid square obstacle used inside the chamber are aimed to generate turbulence by disrupting the flame propagation with different blockage ratios. A sample of results from six flow configurations are presented and discussed here to highlight the success of the LES based modelling technique. Primary objective of the present work is the application of DFSD model in predicting the turbulent premixed flame dynamics in a wide range of flow configurations. Influence of the position of baffle plates with respect to the origin of ignition, in generating overpressure due to the interactions with deflagrating flames, is also examined.

Flame Characteristics: Family 1

Family 1 consists of configurations 5-2-1 with progressively increasing number of baffles from one to three and positioned farthest from ignition bottom as shown in Fig. 3.

For this family of configurations LES results of time histories of overpressure and flame position compared with experimental data are shown in Fig. 11 (a) & (b) respectively. It is evident from Fig. 11(a) that the predicted overpressure trend is in excellent agreement with data with slight under-prediction of peak pressure in all three configurations. Figure 11(a) also highlights the impact of the number of baffles and their position with respect to distance from the ignition bottom. The time elapsed in reaching the first baffle from the ignition bottom and increase in the steepness of pressure gradient due to the generated turbulence can be noticed. For example Configuration 1 which has three obstacles results in the highest peak pressure. LES predicted flame position shown in Fig. 11(b) also compare well with data except for configuration 2 where there is a slight discrepancy. It should be noted that in the case of experiments, the flame position is extracted from high speed video images by locating the farthest location of the flame front from ignition bottom end. From LES calculations, the flame position is obtained by locating the farthest location of the leading edge of the flame front from the bottom end (defined here as the most downstream location of the flame, where c = 0.5 from the ignition point).

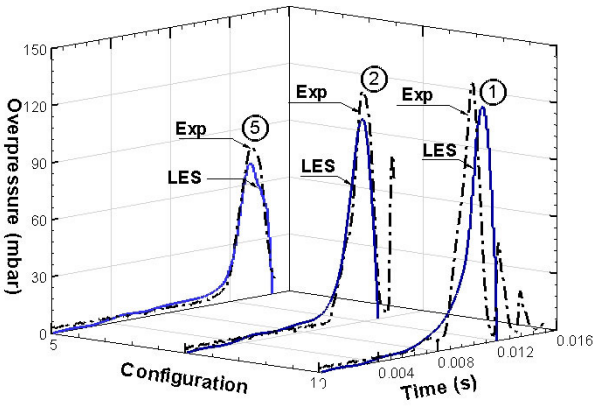

(a)

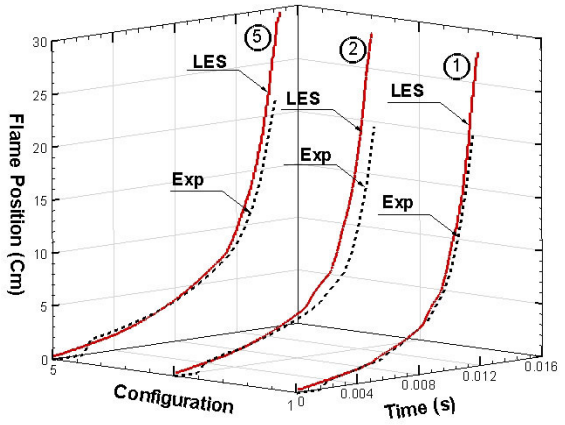

(b)

Figure 11. Comparison of predicted and measured time traces of Family 1 (a) overpressure (b) flame position.

Figures 12 (a) and (b) show comparison of flame speed and acceleration respectively from LES and experiments. It can be seen that the flame speed and acceleration from LES are in very good agreement with experimental measurements, except when the flame is located downstream of the square obstacle in blow-down region. One main reason for this is due to the limitation in the resolution of experimental measurements. Within blow-down region, the flow conditions are highly turbulent and flame propagates faster with approximately about 80-100 m/s in this family.

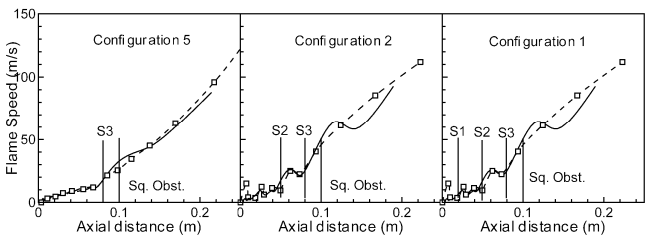

(a)

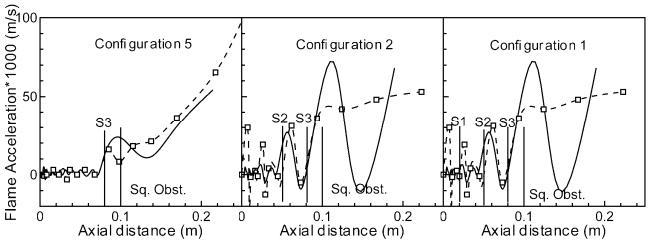

(b)

Figure 12. Comparisons of predicted (Solid line) and measured (Dashed lines with square symbols) (a) flame speed (b) flame acceleration The location of baffle stations (S1, S2 and S3) and the square solid obstacle are shown.

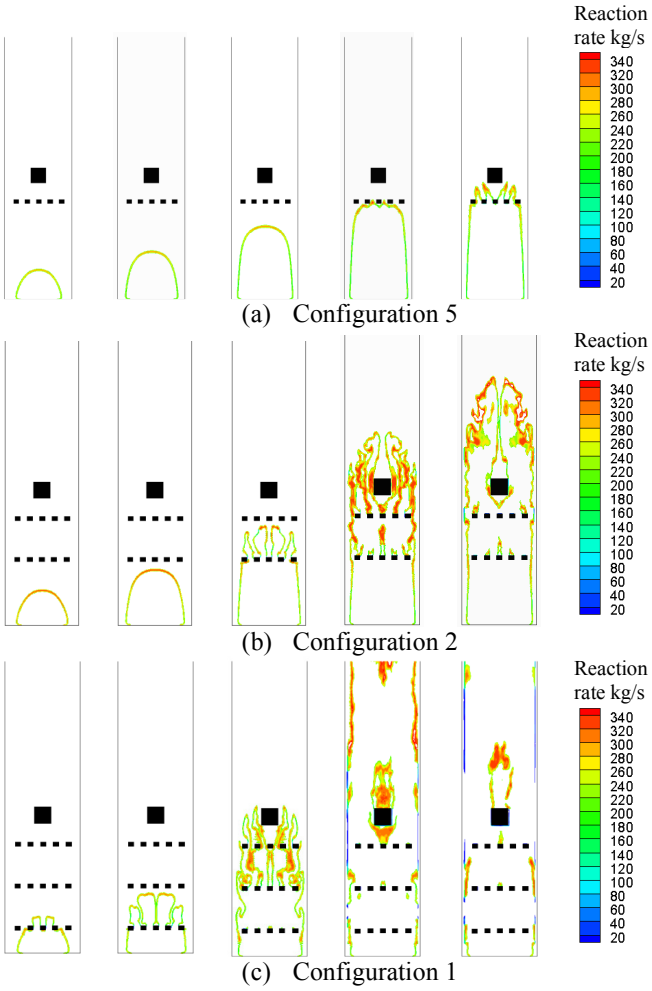

(a) Configuration 5

(b) Configuration 2

(c) Configuration 1

Figure 13. Predicted flame structure in each configuration at times 6, 8, 10, 11.5 and 12.0 ms after ignition.

Figure 13 (a-c) presents cut-views of LES predicted reaction rate contours, showing flame structure at 6.0, 8.0, 10.0, 11.5 and 12.0 ms after ignitions for this family. This facilitates qualitative and quantitative comparison of flame position and its structure at any given time within this family. For instance at 8.0 ms from ignition Figure 13 (c) illustrates the finger shaped flame structure, which is generally expected in chambers having l/d ratio greater than 3. Fig. 13(b) at 11.5 and 12.0 ms shows a clear picture of entrapment of unburnt fuel/air mixture around solid square obstacle within the recirculation zone. Similar pockets or traps in the case of configuration 1 in Fig. 13(c) at times 10.0 and 11.5 ms are clearly noticeable. Similarly, Fig. 13(c) at 11.5 and 12.0 ms shows the consumption of trapped mixture, once the main flame had left the chamber. Comparison of plots gives an insight into how flame acceleration occurs and it could be used to explain how overpressure is generated in a given configuration.

Flame characteristics: Family 3

Family 3 has three configurations i.e. 2-3-4 with two baffle plates at different stations and a solid square obstacle at the fixed position. Figure 14 (a) and (b) shows characteristic comparison of overpressure and flame position respectively for these three configurations, and experimental measurements and LES simulations are compared. It is evident from Fig. 14 (a) that the rate of pressure rise and its trend including first hump are predicted well except for configuration 4, where the computed rate of increase of pressure is slower than measurements indicating a faster decay of turbulence between the second baffle plate and the square obstacle. Figure 14 (b) shows the flame position predictions. Very good agreement can be seen for all configurations. In configuration 3 predictions overlaps with the experimental data and a slightly faster propagation rate across the chamber is seen in configurations 2 and 4. It should be noted here that this phenomenon is only observed in the last few milliseconds of propagation where the flame is experiencing the highest levels of turbulence.

Figure 15 (a) and (b) show comparison between experimental measurements and numerical predictions of flame speed and acceleration. Figure 15 also shows the position of baffle plates and the solid square obstacle to identify the influence of the obstacles. The predictions capture the correct trend and behaviour seen in the experimental data. Highest flame speed and acceleration are recorded at the square obstacle in configuration 2 than other two configurations. It is also interesting to note that, in configuration 4, the slowdown in flame speed and acceleration between the second baffle plate and the square obstacle is due to relatively longer distance compared to other configurations in this family (see Fig. 3).

Figure 16 (a-c) shows the reaction rate contours at various instances in this group. At 6ms, the flame is seen to be jetting out of the first baffle in configurations 3 and 4. In contrast at 6ms, the flame in configuration 2 is seen to be relatively smooth. Similarly, the flame in configuration 2 and 3 can be seen to be interacting with baffle plate at S3 having a different flame structure at 10ms. Figures 16 illustrates quicker flame exit in configuration 4 than in configuration 2. Though, the flame in configuration 2 propagates at lower speed at the beginning, it becomes highly turbulent due to jetting and contortion through repeated baffles. In configuration 3, the flame is found to be distorted as it reaches the first baffle. However, re-laminarisation of the flame between S1 and S3 results in approaching the square obstacle at a later stage compared to configuration 4. These flame interactions results in

the changes in flame speed and contribute to the pressure rise. In general this kind of LES predictions gives a good insight into flame obstacle interactions.

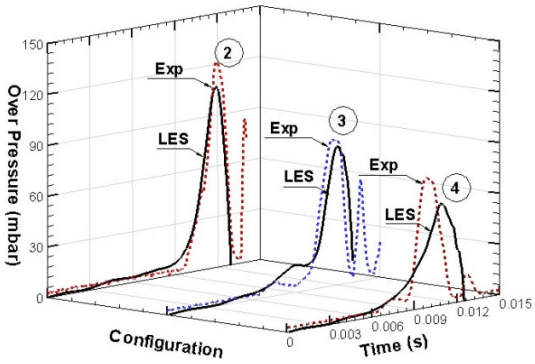

(a)

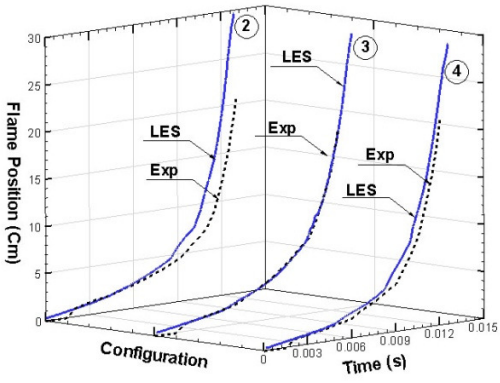

(b)

Figure 14. Family 3: Comparison of predicted and measured (a) overpressure (b) flame position.

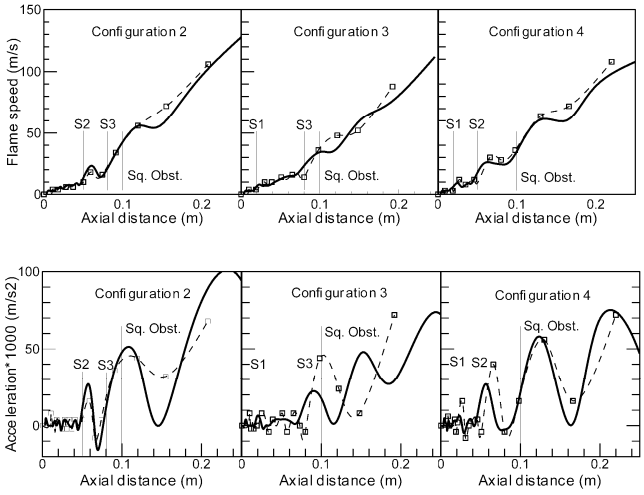

Figure 15. Comparisons of predicted (Solid line) and measured (Dashed lines with square symbols) (a) flame speed (b) flame acceleration The location of baffle stations (S1, S2 and S3) and the square solid obstacle are shown.

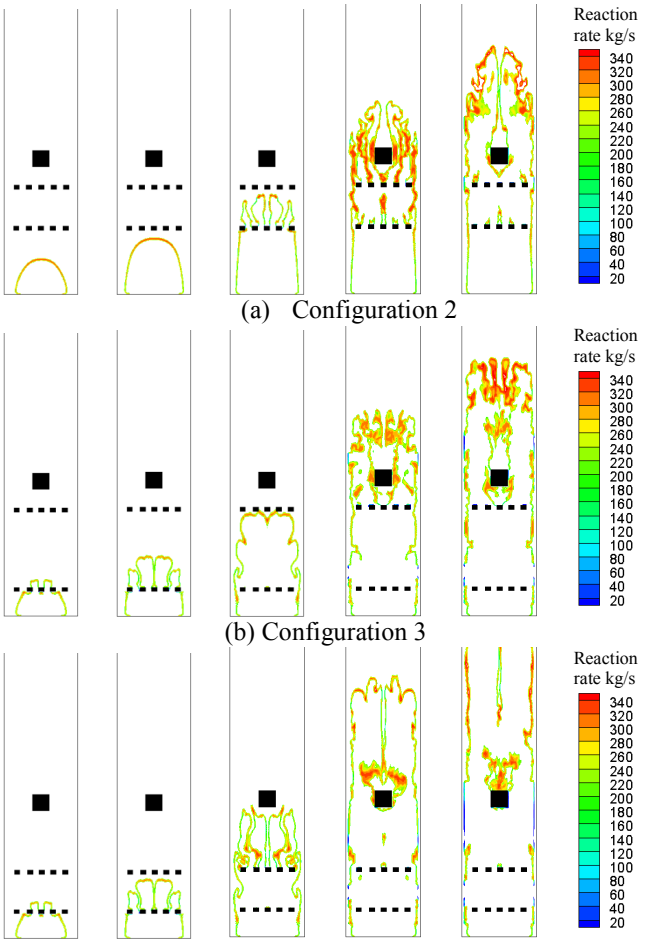

Figure 16. Predicted flame structure in each configuration at times 6, 8, 10, 11.5 and 12.0 ms after ignition.

From the results presented above it can be concluded the novel DFSD model is successful in predicting the flame behaviour, structure; position and other characteristics and they are in agreement with experimental measurements. Generally predicted overpressure-time trend for all configurations are in good agreement with data although slight under-prediction can be seen for some configurations. In all configurations LES results have correctly reproduced experimentally observed flame position, flames speeds, and flame acceleration trends. LES results are also very useful in interpreting how obstacles interact with the propagating flame. This investigation demonstrates the effects of placing multiple obstacles at various locations in the path of the turbulent propagating premixed flame. As expected, calculations show that the increase in blockage ratio increases the overpressure, however, with same blockage ratio, the position of solid obstruction with respect to each other and ignition end has a significant impact on the magnitude of the overpressure and spatial flame structure.

CONCLUSION

In this paper we have shown how LES could be applied with appropriate models to compute premixed and non-premixed combustion situations. A complex swirl flame was considered as an example for non-premixed modelling. It was demonstrated that LES based combustion modelling showed very encouraging results in terms of resolving complex features of the swirl flow considered and predicted results showed good agreement with data. A propagating flame over obstacles was considered for the demonstration of premixed combustion modelling. In this work a novel DSFD model was used in the LES modelling. Comparison of results showed excellent agreement with data demonstrating the ability of LES. Overall it could be concluded that LES is a very useful tool for accurate modelling of premixed and non-premixed reacting flows and expected to grow in the future as it could produce an accurate account of the flow and combustion characteristics.

REFERENCES

[1] Sloan, D.G., Smith, P.J. and Smoot, L.D., Modelling of Swirl in Turbulent Flow Systems, Prog. Energy Combust Sci., 12, 163-250, 1986.

[2] Weber, R, Visser, B.M, Boysan, F, Assessment of turbulent modelling for engineering prediction of swirling vortices in the near burner zone, Int. J. Heat and Fluid Flow, 11, 225-238, 1990

[3] Kim, W, Menon. S. and Mongia, H.,1999, Large eddy simulation of a gas turbine combustor flow, Combust. Sci. Tech., 143, 25-63.

[4] Sankaran, V, Menon, S., LES of spray combustion in swirling flows, J. Turbulence, 3, 11-23, 2002

[5] Di Mare, Jones. W. and Menzies. K., Large eddy simulation of a model gas turbine combustor, Combust. Flame, 137(3), 278-294, 2004.

[6] Wall, C.T and Moin, P., Numerical methods for Large eddy simulation of acoustic combustion instabilities, Tech. Rep. TF.91. Stanford University, CA, 2005.

[7] Patel, S.N.D.H, Jarvis, S, Ibrahim S.S. and Hargrave, G.K., An experimental and numerical investigation of premixed flame deflagration in a semiconfined explosion chamber, Proc. Comb. Inst., 29(2), 1849-1854, 2002.

[8] Masri, A.R., Ibrahim, S.S., and Cadwallader, B.J., Experimental Thermal and Fluid Science, 30, 687-702, 2006.

[9] Charlette, F., Meneveau, C., and Veynante, D., A power-law flame wrinkling model for LES of premixed turbulent combustion Part II: Dynamic formulation, Comb. and Flame, 131, 181-197, 2002.

[10] Fureby, C., Pitsch, H., Lipatnikov and Hawkes, E., A fractal flame-wrinkling large eddy simulation model for premixed turbulent combustion, Proc. of the Combustion Institute, 30(1), 593-601, 2005.

[11] Knikker, R., Veynante, D., and Meneveau, C., Proc. Combust. Inst., 29, 2105-2111, 2002.

[12] Pitsch, H., A consistent level set formulation for large-eddy simulation of premixed turbulent combustion, Combustion and Flame, 143(4), 587-598, 2005.

[13] Smagorinsky, J., General circulation experiments with the primitive equations, Monthly Weather Review, 91(3), 99-164, 1963.

[14] Piomelli, U. and Liu, J., Large eddy simulation of channel flows using a localized dynamic model, Phy. Fluids, Vol. 7, pp. 839-848, 1995.

[15] Moin, P., Squires, K., Cabot, W., and Lee, S., A dynamic subgrid-scale model for compressible turbulence and scalar transport. Physics of Fluids, A3, 2746–2757, 1991.

[16] Branley, N and Jones,W.P., Large eddy simulation of a turbulent non-premixed flame, Comb. Flame, 127, 1914-1934, 2001.

[17] Pitsch, H., 1998, A C++ computer program for 0-D and 1-D laminar flame calculations, RWTH, Aachen.

[18] Malalasekera, W., Ranga-Dinesh, K.K., Ibrahim, S. and A.R.Masri, LES of Recirculation and Vortex Breakdown of Swirling Flames, Comb. Sci. Tech., Vol. 180, pp. 809-832, 2008.

[19] Lockwood, F. C. and Shah, N. G., A New radiation Solution method for Incorporation into General Combustion Prediction Procedures, 18th Symp. (Int.) on Comb., The Combustion Institute, 1405-1414, 1981.

[20] Malalasekera, W. and James, E.H., Radiative Heat Transfer Calculations in Three-Dimensional Complex Geometries, J. of Heat Transfer, 118, 225-228, 1996.

[21] Henson, J.C. and Malalasekera, W., Comparison of discrete transfer and Monte-Carlo methods for radiative heat transfer in three-dimensional non-homogeneous scattering media, Num. Heat Transfer Part A: Applications, 32(1), 19-36, 1997.

[22] Truelove, J. S., 1976, A Mixed Grey Gas Model for Flame Radiation, AERE Harwell, Oxfordshire, UK.

[23] Veynante, D., and Poinsot, T., Large eddy simulations of the combustion instabilities in turbulent premixed burners. Annual research briefs, Center for turbulence research. 253-275, 1997.

[24] Gubba, S.R., Ibrahim, S.S., Malalasekera, W. and Masri, A.R., LES modelling of premixed deflagrating flames in vented explosion chamber with a series of solid obstructions, Comb. Sci. Tech., 10 (180), 1936-1955, 2008.

[25] Ibrahim, S.S, Gubba, S.R., Masri, A.R. and Malalasekera, W., Calculations of Explosion Deflagrating Flames using a Dynamic Flame surface density Model, a Journal of Loss Prevention in the Process Industries, 22(3), 258-264, 2009.

[26] Knikker, R., Veynante, D. and Meneveau, C., A dynamic flame surface density model for large eddy simulation of turbulent premixed combustion, Physics of Fluids, 16(11), L91-L94, 2004.

[27] Al-Abdeli, Y.M., Masri, A.R., Stability characteristics and flow fields of turbulent non-premixed swirling flames, Combust. Theory Modelling 7: 731-766, 2003.

[28] Masri, A.R..Kalt, P.A.M, and Barlow, R.S. The compositional structure of swirl stabilised turbulent non-premixed flames,Combust. Flame 137: 1-37, 2004.

[29] Kent, J. E., Masri, A. R., and Starner, S. H., 2005, A new chamber to study premixed flame propagation past repeated obstacles, Paper presented at the 5th Asia-Pacific Conference on Combustion, The University of Adelaide, Adelaide, Australia, 2005.

[30] Hossain, M., Jones, J.C. and Malalasekera, W., Modelling of a Bluff-Body Nonpremixed Flame Using A Coupled Radiation/Flamelet Combustion Model, Flow Turb. and Combustion, 67, 217-234, 2001.

[31] Ravikanti-Veera, M.M.R, Malalasekera, W. and Hossain, M., Flamelet Based NOx-Radiation Integrated Modelling of Turbulent Non-premixed Flame using Reynolds-stress Closure, Flow, Turbulence and Combustion, 81 (1/2), 609-612, 2008.